

FIGURE 3. Midpoint-rooted neighbor-joining tree reconstructed from variation in the rpoB B gene. Kimura 2-parameter distances were calculated for each pair of sequences. The percentage of bootstrap replicates ($n = 1,000$) in which a given node was recovered is indicated. Five hundred base pairs of the rpoB gene were sequenced from *Sarcocystis* sp. and from representatives of *S. neurona*, *S. falcatula*, and *S. lindsayi* in the sea otter (see Table I for details on isolates). The *Neospora caninum* and *Toxoplasma gondii* homologs were obtained from GenBank (accession nos. AF095904 and AF138960, respectively).

a polymerase chain reaction (PCR) by using degenerate primers designed to amplify the rpoB gene, encoded by the plastid genome of apicomplexans—primers F1 (5'-gcg gtc cca aaa ggg tca gtg gat atg atw twt gaa gat gc) and R3 (5'-gcg gtc cca aaa ggg tca gtc ctt tat ktc cat rtc t). The resulting 504-bp PCR products were directly sequenced using BigDye chemistries and an ABI 3100 automated fluorescent sequencer. Homologous sequences were characterized from isolates of *S. neurona*, *S. falcatula*, and *S. lindsayi*, the origins of which are summarized in Table I. These were aligned to each other and to homologs from *Neospora caninum* and *Toxoplasma gondii* by using CLUSTAL W 1.8 (Thompson et al., 1994), available on the bioinformatics server of the Baylor College of Medicine. Relationships of these sequences were investigated by constructing a gene genealogy by calculating Kimura 2-parameter distances from 1,000 bootstrap replicates of the alignment and using the Neighbor-Joining algorithm using MEGA 2.1 (Kumar et al., 2001).

The rpoB sequence obtained from the otter isolate was placed as a basal member of a clade that also contained the other examined isolates belonging to *Sarcocystis* but that included neither *N. caninum* nor *T. gondii* (Fig. 3). Concordant topologies were obtained when the minimum evolution and maximum parsimony criteria were used (data not shown). Several nucleotide substitutions distinguish this otter specimen from the isolates representing other species of *Sarcocystis*. In contrast, the rpoB of isolates representing *S. falcatula* are comparatively homogeneous. Thus, morphological and genetic evidence indicates that sea otters, in addition to being at the risk of exposure to *S. neurona* parasites, serve as host to at least 1 other species of parasites belonging to the genus *Sarcocystis*.

LITERATURE CITED

DUBEY, J. P., D. S. LINDSAY, D. FRITZ, AND C. A. SPEER. 2001. Structure of *Sarcocystis neurona* sarcocysts. *Journal of Parasitology* **87**: 1323–1327.

- _____, _____, C. E. KERBER, N. KASAI, H. F. J. PENA, S. M. GENNARI, O. C. H. KWOK, S. K. SHEN, AND B. M. ROSENTHAL. 2001. First isolation of *Sarcocystis neurona* from the South American opossum, *Didelphis albiventris*, from Brazil. *Veterinary Parasitology* **95**: 295–304.
- _____, _____, B. M. ROSENTHAL, C. E. KERBER, N. KASAI, H. F. PENA, O. C. KWOK, S. K. SHEN, AND S. M. GENNARI. 2001. Isolates of *Sarcocystis falcatula*-like organisms from South American opossums *Didelphis marsupialis* and *Didelphis albiventris* from Sao Paulo, Brazil. *Journal of Parasitology* **87**: 1449–1453.
- _____, _____, W. J. A. SAVILLE, S. M. REED, D. E. GRANSTROM, AND C. A. SPEER. 2001. A review of *Sarcocystis neurona* and equine protozoal myeloencephalitis (EPM). *Veterinary Parasitology* **95**: 89–131.
- _____, B. M. ROSENTHAL, AND S. SPEER. 2001. *Sarcocystis lindsayi* n. sp. (Protozoa: Sarcocystidae) from the South American opossum, *Didelphis albiventris* from Brazil. *Journal of Eukaryotic Microbiology* **48**: 595–603.
- _____, A. C. ROSYPAL, B. M. ROSENTHAL, N. J. THOMAS, D. S. LINDSAY, J. F. STANEK, S. M. REED, AND W. J. A. SAVILLE. 2001. *Sarcocystis neurona* infections in sea otter (*Enhydra lutris*): Evidence for natural infections with sarcocysts and transmission of infection to opossums (*Didelphis virginiana*). *Journal of Parasitology* **87**: 1387–1393.
- _____, C. A. SPEER, AND R. FAYER. 1989. *Sarcocystosis* of animals and man. CRC Press, Boca Raton, Florida, 215 p.
- KUMAR, S., K. TAMURA, I. B. JAKOBSEN, AND M. NEI. 2001. MEGA2: Molecular evolutionary genetics analysis software. *Bioinformatics* **17**: 1244–1245.
- LINDSAY, D. S., N. J. THOMAS, AND J. P. DUBEY. 2000. Biological characterization of *Sarcocystis neurona* from a Southern sea otter (*Enhydra lutris nereis*). *International Journal for Parasitology* **30**: 617–624.
- _____, _____, A. C. ROSYPAL, AND J. P. DUBEY. 2001. Dual *Sarcocystis neurona* and *Toxoplasma gondii* infection in a Northern sea otter from Washington state, USA. *Veterinary Parasitology* **97**: 319–327.
- MILLER, M. A., P. R. CROSBIE, K. SVERLOW, K. HANNI, B. C. BARR, N. KOCK, M. J. MURRAY, L. J. LOWENSTINE, AND P. A. CONRAD. 2001. Isolation and characterization of *Sarcocystis* from brain tissue of a free-living southern sea otter (*Enhydra lutris nereis*) with fatal meningoencephalitis. *Parasitology Research* **87**: 252–257.
- ROSONKE, B. J., S. R. BROWN, S. J. TORNUST, S. P. SNYDER, M. M. GARNER, AND L. L. BLYTHE. 1999. Encephalomyelitis associated with a *Sarcocystis neurona*-like organism in a sea otter. *Journal of the American Veterinary Medical Association* **215**: 1839–1842.
- THOMPSON, J. D., D. G. HIGGINS, AND T. J. GIBSON. 1994. CLUSTAL W: Improving the sensitivity of progressive multiple sequence alignment through sequence weighting, positions-specific gap penalties and weight matrix choice. *Nucleic Acids Research* **22**: 4673–4680.

J. Parasitol., 89(2), 2003, pp. 399–402
© American Society of Parasitologists 2003

Morphology Is Not a Reliable Tool for Delineating Species Within *Cryptosporidium*

Abbie Fall, R. C. Andrew Thompson, Russell P. Hobbs, and Una Morgan-Ryan*, Division of Veterinary and Biomedical Sciences, Murdoch University, Perth, Western Australia 6150, Australia. * To whom correspondence should be addressed.
e-mail: unaryan@central.murdoch.edu.au

ABSTRACT: Within the coccidia, morphological features of the oocyst stage at the light microscope level have been used more than any other single characteristic to designate genus and species. The aim of this study was to conduct morphometric analysis on a range of *Cryptosporidium*

spp. isolates and to compare morphological data between several genotypes of *C. parvum* and a second species *C. canis*, as well as a variation within a specific genotype (the human genotype), with genetic data at 2 unlinked loci (18S ribonucleic deoxyribonucleic acid and HSP

70) to evaluate the usefulness of morphometric data in delineating species within *Cryptosporidium*. Results indicate that morphology could not differentiate between oocysts from *C. parvum* genotypes and oocysts from *C. canis*, whereas genetic analysis clearly differentiated between the two. The small size of the *Cryptosporidium* spp. oocyst, combined with the very limited characters for analysis, suggests that more reliance should be placed on genetic differences, combined with biological variation, when delineating species within *Cryptosporidium*.

Taxonomic classification for parasitic protozoa is currently based on multiple phenotypic characters such as morphological features detected by light or electron microscopy, unique life cycles, and host specificity (Fayer et al., 2000). For coccidia, morphological features of the oocyst stage at the light microscope level have been used more than any other characteristic to designate genus and species (Morgan, Xiao et al., 1999).

There has been considerable confusion regarding the taxonomy of the genus *Cryptosporidium*, and currently 10 species are regarded as valid. These include *C. parvum* from many mammals, *C. muris* from mice, *C. andersoni* from ruminants, *C. felis* from cats, *C. canis* from dogs, *C. wrairi* from guinea pigs, *C. meleagridis* and *C. baileyi* from birds, *C. serpentis* from snakes and lizards, and *C. saurophilum* from lizards (Fayer et al., 2000, 2001).

Since Tyzzer's first description in 1912, oocysts corresponding in size and shape to *C. parvum* have been described in over 152 different host species (Fayer et al., 2000). Oocysts of *C. parvum* of bovine origin have been described as having a size range of 4.5–5.4 × 4.2–5.0 μm (mean 5.0 × 4.5 μm) and a shape index of 1.1 (Upton and Current, 1985). Few studies have conducted morphometric analysis on *C. parvum* oocysts from a range of hosts. However, molecular data at numerous unlinked loci have provided evidence for substantial genetic variation within what is termed as the *C. parvum* group. Currently, at least 8 different genotypes have been identified within the *C. parvum* group, including the human, cattle, mouse, pig, ferret, and marsupial genotypes, which are genotypically different but morphologically similar (Xiao et al., 2000). This raises the question of whether morphological analysis is a reliable tool for delineating species of *Cryptosporidium*. The aim of this study was to conduct morphometric analysis on a range of *Cryptosporidium* spp. isolates and to compare morphological data between several genotypes of *C. parvum* and a second species *C. canis*, as well as a variation within a specific genotype (the human genotype), with genetic data at 2 unlinked loci to evaluate the usefulness of morphometric data in delineating species within *Cryptosporidium*.

Cryptosporidium spp. oocysts from fresh stool samples from humans, cattle, marsupials, and dogs were purified using phosphate-buffered saline (PBS)-ether and Ficoll® density centrifugation (Meloni and Thompson, 1996). Isolates were genotyped by sequence analysis of the 18S rDNA and HSP 70 loci, using previously described methods (Morgan et al., 1997, 2001). Nucleotide sequences were aligned using Clustal X (Thompson et al., 1997). Distance-based analysis was performed us-

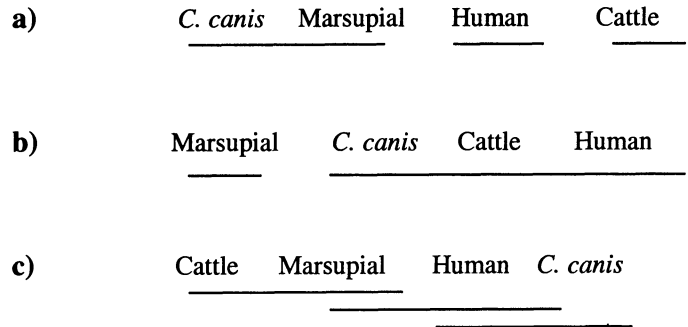


FIGURE 1. Groupings of *Cryptosporidium* species and genotypes determined by Scheffé test. **a.** Groupings based on mean length. **b.** Groupings based on mean width. **c.** Groupings based on mean shape ratio. Underlining joins isolates that are similar, and those significantly different are not joined.

ing Kimura's distance. Trees were constructed using the neighbor-joining algorithm. Bootstrap analyses were conducted using 1,000 replicates. Phylograms were drawn using the TreeView program (Page, 1996).

Cryptosporidium oocysts were measured using the Optimus Image Analysis Package version 5.2 at ×1,000 magnification. The area of analysis was set to enclose each individual oocyst in order to minimize computational time. Threshold was optimized by eye to differentiate the oocyst background. Once the optimal threshold was reached, the software was set to recognize the oocyst as an area object. All measurements (length, width, area, and circularity) were transferred to Microsoft Excel. Statview version 4.0 (Abacus Concepts Inc., Berkeley, California) was used to perform an analysis of variance (ANOVA) with these data. A multiple range test (Scheffé test) at a significance level of 0.05 was then carried out to group the isolates based on differences in their means from the ANOVA.

Significant differences were identified in oocyst length ($P < 0.001$), width ($P < 0.001$), and shape ratio ($P < 0.001$) for human, cattle, and marsupial genotypes of *C. parvum* and *C. canis* in the stub column of Table I. However, a Scheffé test failed to group *C. canis* separately from the *C. parvum* genotypes (Fig. 1).

Smaller, yet significant differences, also were noted in oocyst length ($P < 0.005$), width ($P < 0.001$), and shape ratio ($P < 0.001$) from different isolates within the *C. parvum* human genotype (Table I). The Scheffé test depicts the differences between the human genotype isolates as shown in Figure 2.

Phylogenetic analysis at the 18S rDNA and HSP 70 loci grouped *C. canis* separately and clearly demonstrated that the *C. parvum* group is polyphyletic because *C. wrairi* and *C. meleagridis* were placed within

TABLE I. Morphometric analysis of *Cryptosporidium* oocysts.

Code	Species, genotype	Oocyst length (mean) (μm)	Oocyst width (mean) (μm)	Oocyst shape index (mean) (L/W)*	Oocyst count
AusDog1	<i>C. canis</i>	5.1–4.6 (4.8)	4.6–3.8 (4.2)	1.10–1.21 (1.14)	50
S26	<i>C. parvum</i> , cattle	5.5–5.0 (5.2)	5.0–3.7 (4.3)	1.10–1.35 (1.20)	40
K2	<i>C. parvum</i> , marsupial	5.1–4.5 (4.9)	5.0–3.8 (4.3)	1.02–1.18 (1.14)	40
H22	<i>C. parvum</i> , human	5.5–4.6 (5.0)	4.7–3.8 (4.2)	1.17–1.21 (1.19)	50
H54	<i>C. parvum</i> , human	5.7–4.5 (5.1)	4.7–3.7 (4.2)	1.21–1.21 (1.21)	50
H65	<i>C. parvum</i> , human	5.4–4.3 (4.8)	4.6–3.8 (4.2)	1.17–1.13 (1.14)	50
H79	<i>C. parvum</i> , human	5.5–4.4 (4.9)	4.7–3.8 (4.3)	1.17–1.16 (1.14)	50
H136	<i>C. parvum</i> , human	5.6–4.5 (5.0)	4.6–3.7 (4.2)	1.20–1.20 (1.20)	50
H139	<i>C. parvum</i> , human	5.4–4.6 (5.0)	4.7–3.8 (4.2)	1.15–1.21 (1.19)	50
H156	<i>C. parvum</i> , human	5.6–4.5 (5.0)	4.7–3.9 (4.3)	1.19–1.15 (1.16)	50
H41625	<i>C. parvum</i> , human	5.3–4.7 (5.0)	4.8–3.9 (4.4)	1.10–1.2 (1.13)	50

* L, length, W, width.

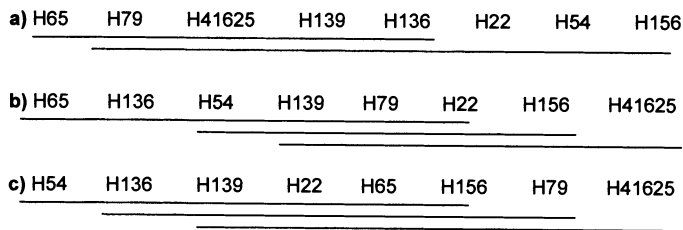


FIGURE 2. Groupings of *Cryptosporidium parvum* human genotypes determined by Scheffé test. **a.** Groupings based on mean length. **b.** Groupings based on mean width. **c.** Groupings based on mean shape ratio. Underlining joins isolates that are similar, and those significantly different are not joined.

this group, providing strong support that the *C. parvum* marsupial genotype is also a distinct species. The *C. parvum* cattle genotype grouped separately from the *C. parvum* human genotype isolates, which were all genetically identical at both loci (Fig. 3). Bootstrap analysis of the data provided strong support for these groupings (Fig. 3).

Cryptosporidium canis is a recognized species because of its apparent host specificity and genetic distinction at numerous loci (Fayer et al., 2001). The *C. canis* isolate used in this study was genetically identical at the loci examined to the isolates used in the study by Morgan, Xiao et al. (2000) and Fayer et al. (2001). As seen in the study by Fayer et al. (2001), this isolate could not be distinguished from the oocysts of different *C. parvum* genotypes by morphological analysis. This overlap in size range between valid species of *Cryptosporidium* is not confined to *C. canis*. *Cryptosporidium meleagridis* and *C. wrairi* also overlap in size with *C. parvum* of bovine origin and are morphologically very similar (Vetterling et al., 1971; Fayer et al., 2000), but they are genetically and biologically distinct and have different host ranges (Fayer et al., 2000).

There is also biological evidence that marsupial, cattle, and human genotypes may be separate species. The marsupial genotype appears to be host specific and is not infectious to nude mice (Morgan, Xiao et al., 1999; Xiao et al., 2000). The human and cattle genotypes have been shown to be genetically distinct at a wide range of loci, and they also exhibit differences in host specificity because the human genotype appears to be confined largely to humans, whereas the cattle genotype infects a wide host range (Morgan, Xiao et al., 1999; Xiao et al., 2000). Differences in growth rates in *in vitro* culture (Hijjawi et al., 2001) as well as fundamental differences in ribosomal gene expression (Le Blancq et al., 1997) also have been reported. In addition, genetic recombinants between the human and cattle genotypes have never been detected despite the fact that both genotypes can infect humans and coinfections have been reported to occur (Patel et al., 1988).

In this study the *C. parvum* cattle genotype oocysts (isolate S26) had a size range of 5.5–5.0 × 5.0–3.7 μm (mean 5.2 × 4.3 μm) and a shape index of 1.20. Other authors have reported a size range of 4.7–6.0 × 4.4–5.0 μm (mean 5.0 × 4.7 μm) and a shape index of 1.06 (Fayer et al., 2001). Upton and Current (1985) have reported a size range of 4.5–5.4 × 4.2–5.0 μm (mean 5.0 × 4.5 μm) and a shape index of 1.1. Similarly, in this study there was significant variation between different isolates of the *C. parvum* human genotype (see Table I; Fig. 2), yet genetic analysis at 2 loci grouped all the human genotype isolates as identical. Genetic analysis at the hypervariable GP-60 locus also did not reveal any differences between these isolates (U. Morgan-Ryan, unpubl. obs.).

Oocysts of *Cryptosporidium* are among the smallest exogenous stages of the apicomplexans; therefore, all morphological differences may not be clear at light microscope levels. Oocyst measurements are frequently conducted using different types of microscopes, different objectives, and different measuring systems (Morgan, Xiao et al., 1999). Any inaccurate measurement is of great significance because of the small size of the oocyst. The age and storage conditions of the oocyst and the isolation techniques also can affect the shape of the oocyst and its measurement. This makes interlaboratory comparisons very problematic. Morphometric analysis of *Cryptosporidium* is further limited by the lack of distinguishing morphological characters, because there are only 2 characters that can be analyzed (length or width, and shape index). Electron mi-

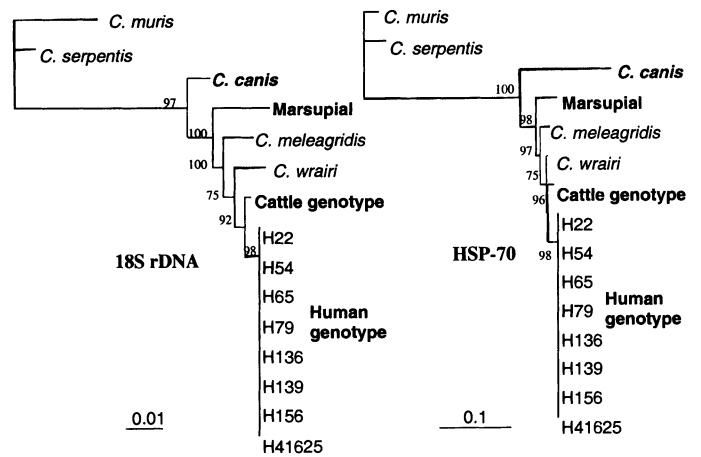


FIGURE 3. Phylogram of *Cryptosporidium* species and genotypes inferred by neighbor-joining analysis of Kimura's distances at the 18S rDNA and HSP 70 gene loci. Percent bootstrap support from 1,000 replicate samples is indicated at the left of the supported node.

croscopy study to distinguish ultrastructural differences is usually not possible because in most cases oocysts are recovered from fecal samples, and tissue sections are not available. Genetic analysis, however, is much more informative than morphological data in the case of *Cryptosporidium* spp. because the number of characters available for analysis is limited only by the size of the genome.

The difficulties of using morphology as a means of delineating species within the Apicomplexa are well known. For example, oocysts of *Toxoplasma gondii* (average size 10 × 11 μm) are disporic with tetrazoid sporocysts and overlap in size and shape with *Hammondia hammondi* and *Neospora caninum*, all of which belong to separate genera (Levine, 1982). A similar problem with the identity of the exogenous stage arose within the species of *Sarcocystis*. When excreted, the weak-walled sporulated oocysts ruptured and released sporocysts that appeared to be identical to sporocysts of other species (Morgan, Monis et al., 1999). Some *Frenkelia* species appear to be identical to *Sarcocystis*, and both genera are differentiated by host specificity and cyst tissue characteristics.

Morphology is an invaluable tool for delineating species in many organisms. However, in the case of *Cryptosporidium* spp. the problems outlined above suggest that it is not a reliable means of delineating species in this genus and that more reliance should be placed on genetic and biological data such as host occurrence when delineating species of *Cryptosporidium*.

LITERATURE CITED

- FAYER, R., U. MORGAN, AND S. J. UPTON. 2000. Epidemiology of *Cryptosporidium*: Transmission, detection and identification. *International Journal for Parasitology* **30**: 1305–1322.
- , J. M. TROUT, L. XIAO, U. MORGAN, A. A. LAL, AND J. P. DUBEY. 2001. *Cryptosporidium canis* n. sp. from domestic dogs. *Journal of Parasitology* **87**: 1415–1422.
- HIJJAWI, N. S., B. P. MELONI, U. M. MORGAN, AND R. C. A. THOMPSON. 2001. Complete development and long-term maintenance of *Cryptosporidium parvum* human and cattle genotypes in cell culture. *International Journal for Parasitology* **31**: 1048–1055.
- LE BLANCQ, S. M., N. K. KHRAMTSOV, F. ZAMANI, S. J. UPTON, AND T. WU. 1997. Ribosomal RNA gene organisation in *Cryptosporidium parvum*. *Molecular and Biochemical Parasitology* **90**: 463–478.
- LEVINE, D. N. 1982. Taxonomy and lifecycles of coccidia. In *The biology of coccidia*, P. L. Long (ed.). University Park Press, College Park, Maryland, p. 1–33.
- MELONI, B. P., AND R. C. A. THOMPSON. 1996. Simplified methods for obtaining purified oocysts from mice and for growing *Cryptosporidium parvum* *in vitro*. *Journal of Parasitology* **82**: 757–762.
- MORGAN, U. M., C. C. CONSTANTINE, D. A. FORBES, AND R. C. A. THOMPSON. 1997. Differentiation between human and animal iso-

- lates of *Cryptosporidium parvum* using rDNA sequencing and direct PCR analysis. *Journal of Parasitology* **83**: 825–830.
- , P. T. MONIS, R. FAYER, P. DELPAZES, AND R. C. A. THOMPSON. 1999. Phylogenetic relationships among isolates of *Cryptosporidium*: Evidence for several new species. *Journal of Parasitology* **85**: 1126–1133.
- , L. XIAO, R. FAYER, A. A. LAL, AND R. C. A. THOMPSON. 1999. Variation in *Cryptosporidium*: Towards a taxonomic revision of the genus. *International Journal for Parasitology* **29**: 1733–1751.
- , P. MONIS, A. FALL, P. J. IRWIN, R. FAYER, K. DENHOLM, J. LIMOR, A. A. LAL, AND R. C. A. THOMPSON. 2000. *Cryptosporidium* in domestic dogs—The ‘dog’ genotype. *Applied and Environmental Microbiology* **66**: 2220–2223.
- , P. MONIS, L. XIAO, J. LIMOR, S. RAIDAL, P. O’DONOGHUE, R. GASSER, A. MURRAY, R. FAYER, B. BLAGBURN, A. A. LAL, AND R. C. A. THOMPSON. 2001. Molecular and phylogenetic characterisation of *Cryptosporidium* from birds. *International Journal for Parasitology* **31**: 289–296.
- PAGE, R. D. M. 1996. TREEVIEW: An application to display phylogenetic trees on personal computers. *Computer Applications in the Biosciences* **12**: 357–358.
- PATEL, S., S. PEDRAZA-DIAZ, J. MCLAUCHLIN, AND D. P. CASEMORE. 1998. Molecular characterisation of *Cryptosporidium parvum* from two large suspected waterborne outbreaks. *Communicable Diseases and Public Health* **1**: 232–233.
- THOMPSON, J. D., T. J. GIBSON, F. PLEWNIAC, F. JEANMOUGIN, AND D. G. HIGGINS. 1997. The Clustal X windows interface: Flexible strategies for multiple sequence alignment aided by quality analysis tools. *Nucleic Acids Research* **25**: 4876–4882.
- UPTON, S. J., AND W. L. CURRENT. 1985. The species of *Cryptosporidium* (Apicomplexa: Cryptosporidiidae) infecting mammals. *Journal of Parasitology* **71**: 625–629.
- VETTERLING, J. M., H. R. JERVIS, T. G. MERRILL, AND H. SPRINZ. 1971. *Cryptosporidium wrairi* sp. n. from the guinea pig *Cavia porcellus*, with an emendation of the genus. *Journal of Protozoology* **2**: 243–247.
- XIAO, L., U. M. MORGAN, R. FAYER, R. C. A. THOMPSON, AND A. A. LAL. 2000. *Cryptosporidium* systematics and implications for public health. *Parasitology Today* **16**: 287–292.

J. Parasitol., 89(2), 2003, pp. 402–407
© American Society of Parasitologists 2003

Molecular Cloning of a Novel Multidomain Kunitz-Type Proteinase Inhibitor From the Hookworm *Ancylostoma caninum*

John M. Hawdon, Bennett Datu, and Melissa Crowell, Department of Microbiology and Tropical Medicine, The George Washington University Medical Center, 725 Ross Hall, 2300 Eye Street NW, Washington, D.C. 20037. e-mail: mtrmjmh@gwumc.edu

ABSTRACT: Degenerate oligonucleotide primers derived from conserved serine protease inhibitors were used to amplify a 90–base pair (bp) amplicon from an *Ancylostoma caninum* adult-stage complementary deoxyribonucleic acid (cDNA) library by polymerase chain reaction (PCR). The amplicon was labeled and used as a probe to screen the library, and a 2,300-bp cDNA clone was identified. The 5′ end of the molecule was obtained from adult cDNA by 5′-RACE. The complete sequence named *A. caninum* Kunitz-type proteinase inhibitor (*Ac-kpi-1*) was 2,371 bp and encoded a 759–amino acid open reading frame. The deduced amino acid sequence had a calculated molecular weight of 84,886 Da and contained an amino terminal signal peptide, suggesting that the protein is secreted. Analysis of the predicted protein sequence indicates 12 highly conserved Kunitz-type serine protease inhibitor domains connected by short, conserved spacers. On the basis of sequence analysis, the first 11 domains are predicted to be active serine protease inhibitors based on the P1 amino acid. Domains 5–8 have identical amino acid sequences, and the remaining domains are 38–88% identical. Domain 12 lacks several of the conserved cysteine residues and has an atypical amino acid in the P1 position, suggesting that it is nonfunctional. Reverse transcriptase–PCR indicated that the *Ac-kpi-1* messenger ribonucleic acid is present in egg, L₁, L₃, and adult stages but is most abundant in the adult stage. *Ac-KPI-1* is most similar in domain architecture to several extracellular matrix proteins involved in cellular remodeling during insect development. In addition, there are 44 nematode proteins containing one or more Kunitz domains in GenBank, including several with multiple domains.

Many parasitic nematodes release molecules that interfere with host proteases, presumably enabling the parasite to avoid the detrimental effects of proteolysis. For example, hookworms, and possibly other hematophagous nematodes, release anticoagulant peptides, which inhibit the proteases of the host coagulation pathways (Eff, 1966; Cappello et al., 1996), and *Ascaris* releases serine protease inhibitors, which interfere with host digestive enzymes (Martzén et al., 1990).

Kunitz inhibitors (KI) are a class of serine protease inhibitors that include basic pancreatic trypsin inhibitor (Fioretti et al., 1985), tissue factor pathway inhibitor (TFPI) (Wun et al., 1988; Sprecher et al.,

1994), and numerous dendrotoxins and venoms (Dufton, 1985). Kunitz inhibitor domains are characterized by a conserved spacing between cysteine residues (C₈C₁₅C₇C₁₂C₃) and a characteristic disulfide bonding pattern. The inhibitors may comprise a single Kunitz domain or “head” or have several domains separated by variable spacer regions. Recently, a small, single-domain KI has been described from adults of the hookworm *Ancylostoma ceylanicum* (Milstone et al., 2000). In this study, we describe the cloning of a novel KI from adults of the related hookworm *A. caninum*. The *A. caninum* Kunitz-type proteinase inhibitor (*Ac-KPI-1*) complementary deoxyribonucleic acid (cDNA) encodes a large multiheaded protein containing 12 tandem Kunitz domains.

An adult *A. caninum* cDNA library was constructed in vector λ-ZAP II (Stratagene, La Jolla, California) according to standard methods (Hawdon et al., 1995). Phage DNA was isolated from infected bacteria and used as a template in a polymerase chain reaction (PCR), using degenerate primers derived from the conserved serine protease inhibitor sequences (SPI-5′-PstI, 5′-GGTACTGCAGTACGGY CCDTGYAARG-3′ and SPI2-3′-HindIII, 5′-GGTCAAGCTTGTRCCRCARCCRCGTA-3′, where Y = C or T, D = AGT, and R = A or G). Each primer was designed by eye from back-translated Kunitz domain protein sequence and contained a 5′ restriction enzyme sequence (underlined) to facilitate amplicon cloning. A hemi-nested strategy was used in the PCR. In round 1, the forward primer SPI-5′-P was used together with the opposite-flanking λ-ZAP II vector primer (T7 promoter) in a “hot-start” PCR (Arnheim and Erlich, 1992). Ten μl reaction mixtures containing the template and 100 ng of each primer were subjected to a temperature of 94 C for 5 min followed by 85 C for 5 min, after which 10 μl containing buffer, 1.5 mM MgCl₂, 0.2 mM of each deoxynucleotide triphosphate, and 1 U of *Taq* polymerase (Promega, Madison, Wisconsin) was added. The reactions were subjected to 30 cycles of denaturation at 94 C for 1 min, annealing at 37 C for 1 min, and extension at 72 C for 1 min. In second-round PCR, 1 μl of a one-tenth dilution of the first-round reaction was used as template with the forward primer and the nested reverse primer SPI2-3′-HindIII. The reactions were subjected to the same cycles as above, except that the annealing temperature was increased to 42 C.

The hemi-nested PCR strategy yielded a 90–base pair (bp) amplicon,